ISSN 0967-0912, Steel in Translation, 2016, Vol. 46, No. 6, pp. 395–400. © Allerton Press, Inc., 2016.
Original Russian Text © V.P. Dement'ev, S.V. Feiler, D.V. Boikov, N.A. Kozyrev, E.V. Polevoi, 2016, published in Izvestiya Vysshikh Uchebnykh Zavedenii, Chernaya Metallurgiya, 2016, No. 6, pp. 402–408.

Operation of Imported Rail on the East Siberian Railroad

V. P. Dement'ev[a, *], S. V. Feiler[a, *], D. V. Boikov[b, **], N. A. Kozyrev[a, *], and E. V. Polevoi[b, ****]**

[a]*Siberian State Industrial University, Novokuznetsk, Russia*
[b]*OAO EVRAZ Zapadno Sibirskii Metallurgicheskii Kombinat (ZSMK), Novokuznetsk, Russia*
*e-mail: *mchmsis@mail.ru, **Dmitry.Bojkov@evraz.com,*
****kozyrev_na@mtsp.sibsiu.ru, *****Egor.Polevoj@evraz.com*

Received April 28, 2016

Abstract—Japanese R65 rail is metallographically analyzed after operation in the East Siberian Railroad. Its chemical composition complies with Technical Specifications TU 0921-239-01124323–2007 for the steel used in the production of 350LDT rail. The macrostructure of the metal is of satisfactory quality. The tensile mechanical properties, hardness, and impact strength at +20°C determined on samples from the nonoperational chamfer of the rail head are consistent with Technical Specifications TU 0921-239-01124323–2007 for the steel used in the production of 350LDT rail. The impact strength at negative temperatures does meet the corresponding requirements. The content of nonmetallic inclusions is low. However, exogenous inclusions are present at unacceptable levels. The microstructure of the Japanese rail sample consists of sorbite and plate pearlite, whose dispersity declines on moving away from the surface. In operation of the rail, thin inclined cracks (depth 1.1 mm) form at the surface of the working chamfer in the rail head; in addition, lateral wear is considerable (up to 15 mm).

Keywords: rail, rolled steel, nonmetallic inclusions, heat treatment, mechanical properties, working life
DOI: 10.3103/S0967091216060036

Globally, in rail production, various methods are used for thermal hardening: differential quenching by fast water fluxes, compressed air, or a water–air mixture; hardening of the head in polymer solution; and bulk quenching in oil [1–11]. The method chosen greatly affects rail life [12, 13]. Until recently, all of the rail produced at the Nizhny Tagil and Kuznetsk metallurgical plants underwent bulk quenching. In 2010 and 2011, differential quenching by air was introduced at OAO EVRAZ Zapadno SIbirskii Metallurgicheskii Kombinat (OAO EVRAZ ZSMK) and hardening in polymer solution was introduced at OAO Mechel. Imported rail with differential quenching has been in use on OAO RZhD lines since 1995, however. The life of such rail in Siberia and the Far North is of great interest. In the present work, we investigate the quality of Japanese R65 rail after operation on curved sections on the East Siberian Railroad. In Fig. 1, we show a rail template with considerable lateral wear (up to 15 mm). The rails were laid in a 5256-km path on a curved section (radius 297 m). The traffic on the route (gross load) was 136 million t. The rail was removed in April 2013 on account of the lateral wear.

Table 1 compares the composition of the rail steel with Russian requirements.

The sample complies in composition with Technical Specifications TU 0921-230-01124323–2007 for the steel used in the production of 350LDT rail.

The results of fractional gas analysis show that the oxygen content is greatest in calcium aluminates (2.6 ppm) and in alumosilicates, calcium silicates, and magnesium spinels (2.2 ppm) and least in silicates (1.3 ppm).

The macrostructure of the rail cross section, highlighted by etching in 50% hydrochloric acid, is assessed in accordance with reference document RD 14-2R-5–2004. The macrostructure is satisfactory in

Fig. 1. Rail template.

Table 1. Chemical composition of rail

Comparison	Content, %													ppm
	C	Mn	Si	P	S	Cr	Ni	Cu	Al	V	Ti	Mo	N	O_2
Sample	0.78	0.80	0.64	0.016	0.005	0.51	0.02	0.02	0.002	0.003	0.002	0.006	0.0022	4.6
Technical Specifications TU 0921-239-01124323–2007	0.72/0.82	0.70/1.20	0.35/1.00	≤0.025	≤0.020	0.30/0.70	≤0.10	≤0.10	≤0.005	≤0.01	≤0.025	≤0.02	≤0.015	≤20

Minimum/maximum values for steel in 350LDT rail.

Table 2. Tensile mechanical properties and impact strength of rail samples

Sample	σ_y, N/mm^2	σ_u, N/mm^2	δ_5, %	Ψ, %	KCU, J/cm^2, at temperature, °C	
					+20	–60
1 (cut from nonoperational chamfer)	870	1270	12.0	44.0	20 21	4.8
2 (cut from operational chamfer, in crumpling zone)	840	1260	13.0	45.0	12 8.6	4.8
Technical Specifications TU 0921-239-01124323–2007 for 350LDT rail	–	≥1240	≥9.0	–	≥15 (1.5)	–

terms of axial segregation (II), point nonuniformity (II), and segregation bands (III). On templates, thin inclined cracks are seen on the surface of the working chamfer in the head. The network of cracks penetrates to a depth of 1 mm.

The tensile mechanical properties, hardness, and impact strength at +20°C for the contact surface and over the head cross section are determined in accordance with State Standard GOST R 51685–2000 and Technical Specifications TU 0921-239-01124323–2007. The impact strength of two samples is tested at –60°C. Tables 2 and 3 present the mechanical test data and hardness, respectively. The tensile mechanical properties, hardness, and impact strength at +20°C for samples cut from the nonoperational chamfer of the rail head are consistent with Technical Specifications TU 0921-239-01124323–2007 for the steel used in the production of 350LDT rail.

The elevated hardness at the head's contact surface (404 *HB*) and the reduced impact strength at +20°C (8.6–12.0 J/cm^2) for samples cut from the operational chamfer of the rail head are due to cold hardening of the metal surface in operation. The impact strength at –60°C is low: 4.8 J/cm^2. These results indicate that rails reliable at low temperature cannot be produced by differential quenching [14, 15].

To determine the tensile mechanical properties and impact strength at the base of the rail, fracture and

Table 3. Hardness of rail samples

Comparison	Hardness *HB*							
	head					web	base	
	contact surface	10 mm	chamfer		22 mm			
Sample	404	380	378	–	347	325	339	329
Technical Specifications TU 0921-239-01124323–2007 for 350LDT rail	362–400	≥341	≥341	≥341	≥341	≤341	≤363	

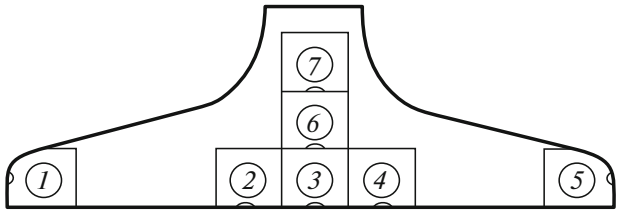

Fig. 2. Position of samples in rail base.

impact samples are cut as in Fig. 2. The test results are presented in Table 4.

The greatest strength (σ_y = 860 N/mm^2, σ_u = 1260 N/mm^2) is observed for samples cut from the bottom of the base at the vertical axis (sample 3); these results are comparable with the values in the head (σ_y = 840–870 N/mm^2, σ_u = 1260–1270 N/mm^2), The plasticity for sample 3 in the base (δ_5 = 9.5%, ψ = 36%) is somewhat less than for the head (δ_5 = 12–13%, ψ = 44–45%).

The strength at some distance from the vertical axis (samples 2 and 4) is somewhat lower (σ_y = 780 N/mm^2, σ_u = 1200–1220 N/mm^2). The corresponding values for ψ are 28 and 40% for samples 2 and 4, respectively; those for δ_5 are 9.9 and 11%, respectively.

For sample 1, with relatively low strength (σ_y = 630 N/mm^2, σ_u = 1020 N/mm^2), we find that ψ = 58%; for sample 5, the strength is somewhat higher (σ_y = 730 N/mm^2, σ_u = 1200 N/mm^2), while ψ = 34%. For samples 1 and 5, δ_5 = 12%.

For samples 6 and 7 on the vertical axis, the strength (σ_y = 670–750 N/mm^2, σ_u = 1090–1160 N/mm^2) and plasticity (δ_5 = 9.5–10.5%, ψ = 23–25%) are somewhat reduced.

The impact strength at +20°C is mainly in the range 15–23 J/cm^3 for samples in the base; in two cases, it is 12 J/cm^2; in two, it is comparable with that in the head (9.6–9.8 J/cm^3).

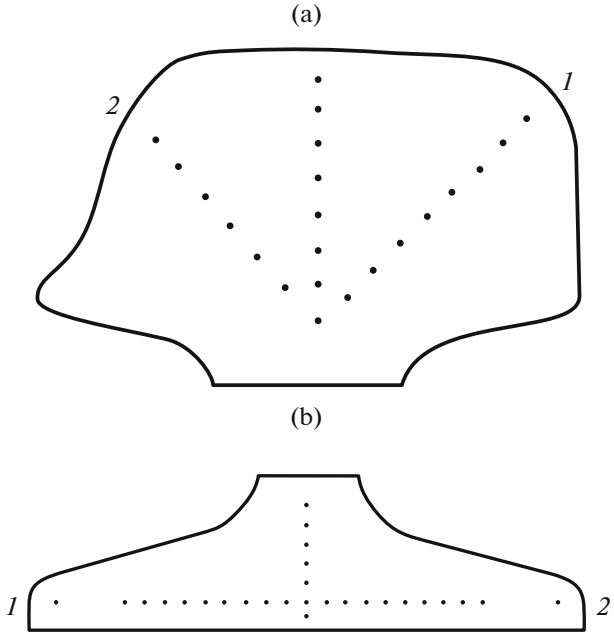

Fig. 3. Points of hardness measurement in the head (a) and base (b).

The impact strength at –60°C is relatively low (3.6–9.7 J/cm^2). The best values are found at the edges (samples 1 and 5): 9.7 and 17 J/cm^3.

The hardness over the cross section is measured by the Rockwell method on an AFFRI 251 VRSD instrument. In the head, measurements are made over the vertical axis from the contact surface to a depth of 40 mm and from the chamfers at an angle of 45° to the horizontal, at intervals of 5.0 mm, starting at a depth of 10 mm (Fig. 3a). In the base, the hardness is measured along the vertical axis to a depth of 35 mm and along a horizontal line passing through the control point, at intervals of 5.0 mm (Fig. 3b). The results for the head and base are shown in Tables 5 and 6, respectively. The hardness in the head declines on moving away from the surface.

Table 4. Mechanical characteristics over the rail cross section

Sample	σ_y, N/mm^2	σ_u, N/mm^2	δ_5, %	Ψ, %	KCU, J/cm^2, at temperature, °C	
					+20	–60
1 (edge)	630	1020	12.0	58.0	23, 23	9.7
2	780	1200	9.9	28.0	23, 19	3.6
3	860	1260	9.5	36.0	15, 18	3.6
4	780	1220	11.0	40.0	12, 9.8	4.8
5 (edge)	730	1200	12.0	34.0	23, 18	17
6	750	1160	9.5	23.0	9.6, 20	7.2
7	670	1090	10.5	25.0	12, 15	6.0

Table 5. Hardness *HRC* (*HB*) in the head

Direction of measurement	Hardness *HRC* (*HB*) at a distance, mm, from the surface								
	5	10	15	20	25	30	35	40	45
Vertically	37.3 (361.7)	37.1 (359.9)	36.8 (357.2)	36.3 (352.7)	34.2 (333.8)	33.3 (325.7)	32.7 (321.4)	32.9 (322.1)	–
From nonoperational chamfer *1*	38.2 (369.5)	38.1 (368.9)	37.1 (359.9)	36.1 (350.9)	35.2 (342.8)	35.2 (342.8)	34.1 (330.7)	33.3 (325.7)	32.9 (322.1)
From operational chamfer *2*	37.7 (355.3)	37.4 (362.6)	36.4 (353.6)	36.9 (358.1)	35.7 (347.3)	35.5 (345.5)	–	–	–

Table 6. Hardness *HRC* (*HB*) in the base

Direction of measurement	Hardness *HRC* (*HB*) at a distance, mm, from the surface													
	5	10	15	20	25	30	35	40	45	50	55	60	65	70
1	34.9 / 334	34.5 / 337	33.1 / 324	33.7 / 329	30.6 / 303	33.1 / 324	29.6 / 295	–	–	–	–	–	–	–
2	33.6 / 328	32.9 / 322	31.7 / 312	30.5 / 302	26.9 / 275	25 / 263	24.6 / 259	24.8 / 261	28 / 283	28.1 / 284	28.8 / 289	27 / 276	28.1 / 284	31.4 / 309
3	33.2 / 325	33.3 / 327	32.9 / 322	31.7 / 312	31.2 / 308	25.2 / 263	24.8 / 261	23.5 / 253	28.1 / 284	27.9 / 282	28.4 / 286	28.1 / 284	28.8 / 288	31.7 / 312

Directions: (*1*) along vertical axis; (*2*) horizontally from the vertical axis to point 1; (*3*) horizontally from the vertical axis to point 2 (Fig. 3).

The hardness at a distance of 25 mm from the vertical axis is 30.5–33.6 *HRC* (302.0–328.4 *HB*); at 40 mm, the values decline to 23.5–25.0 *HRC* (253.0–262.7 *HB*), before rebounding to 31.7 *HRC* (311.6 *HB*).

The hardness at the base surface is also measured on a template of length around 330 mm after surface grinding to a depth of 1 mm. Measurements are made along the rolling direction at 10 mm intervals, starting at one end, in five zones: in the axial zone and at distances of 20 and 40 mm to the left and right of the axis. Table 7 presents the results.

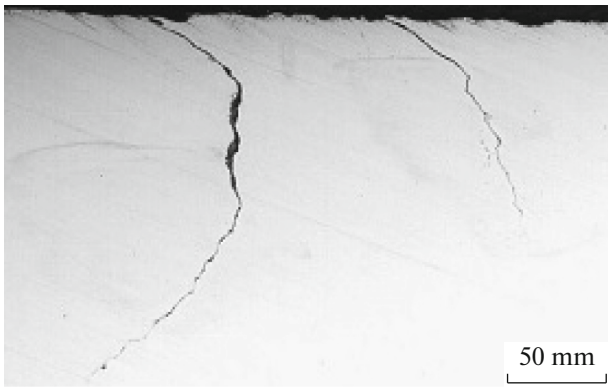

Fig. 4. Cracks in the rail head.

At the sample surface, at a distance of about 250 mm from the end, the hardness in the axial zone and at a distance of 40 mm to the right of the axis is practically the same: 35.2–37.8 *HRC* (342.8–366.2 *HB*). At a distance of 80 mm, we find values of 23.3–29.2 *HRC* (251.8–291.6 *HB*) at all the points considered.

The content of nonmetallic inclusions is assessed on a section cut from the lateral surface of the head. Neither impermissible rows of alumina and titanium nitrides nor rows of alumina and titanium nitrides cemented by silicates are observed. Rows of large complex oxides are also absent. Inspection of the section reveals a single globular inclusion (diameter 10.0 μm). Mainly sulfide threads are seen (size score 1.5 according to State Standard GOST 1778–70). At the individual sulfide inclusions, we encounter a few inclusions of titanium nitrides as pale pink clusters. A single silicate plate (length 135 μm) is observed.

The microstructure of the metal is studied on sections cut from the head, the center of the web, and the center and edges of the base, after etching in 4% alcoholic nitric-acid solution. Inspecting unetched sections from the contact surface of the head, we observe zigzag cracks (depth up to 1.1 mm), as shown in Fig. 4. The cracks are partially filled with uniform gray mass (corrosion products).

After chemical etching in 4% alcoholic nitric-acid solution, structure with deformed grains is observed at the edges of the cracks; no decarburization is seen.

Table 7. Hardness at the bottom surface of the base

Measurement	Hardness *HRC* (*HB*)				
	40 mm to left of axis	20 mm to left of axis	in axial zone	20 mm to right of axis	40 mm to right of axis
1	36.6 (355.4)	37.8 (366.2)	36.8 (357.2)	37.3 (361.7)	35.8 (348.2)
2	36.2 (351.8)	37.6 (364.4)	36.7 (356.3)	36.9 (358.1)	35.7 (347.3)
3	36.0 (350.0)	37.5 (363.5)	36.2 (351.2)	37.2 (360.8)	35.4 (344.6)
4	36.8 (357.2)	37.3 (361.7)	36.0 (350.0)	36.5 (354.5)	35.7 (347.3)
5	36.1 (350.9)	37.3 (361.7)	35.2 (342.8)	37.6 (364.4)	35.9 (349.1)
6	36.4 (353.6)	37.0 (359.)	35.6 (346.4)	36.2 (351.8)	36.1 (350.9)
7	36.2 (351.8)	37.6 (364.4)	35.9 (349.1)	36.0 (350.0)	35.7 (347.3)
8	35.8 (348.2)	37.6 (364.4)	36.0 (350.0)	36.3 (352.7)	35.6 (346.4)
9	35.7 (347.3)	36.5 (354.5)	35.8 (348.2)	36.3 (352.7)	36.1 (350.9)
10	35.8 (348.2)	36.8 (357.2)	35.8 (357.2)	36.8 (357.2)	35.7 (347.3)
11	36.1 (350.9)	36.9 (358.1)	36.5 (354.5)	36.2 (351.8)	35.7 (347.3)
12	36.2 (351.8)	37.0 (359.0)	36.8 (357.2)	37.1 (359.9)	36.0 (350.0)
13	36.1 (350.9)	36.8 (357.2)	36.9 (358.1)	37.4 (362.6)	35.7 (347.3)
14	36.9 (358.1)	37.1 (359.9)	36.0 (350.0)	37.1 (359.9)	36.1 (350.9)
15	36.3 (352.7)	36.8 (357.2)	37.1 (359.9)	36.9 (358.1)	35.9 (349.1)
16	36.9 (358.1)	36.2 (351.8)	36.4 (353.6)	36.8 (357.2)	35.9 (349.1)
17	36.9 (358.1)	37.3 (361.7)	36.6 (355.4)	37.1 (359.9)	35.6 (346.4)
18	36.5 (354.5)	37.3 (361.7)	37.0 (359.0)	36.8 (357.2)	36.0 (350.0)
19	36.8 (357.2)	36.8 (357.2)	37.0 (359.0)	36.5 (354.5)	36.3 (352.7)
20	36.9 (358.1)	37.1 (359.9)	36.8 (357.2)	36.9 (358.1)	35.3 (343.7)
21	36.3 (352.7)	37.0 (359.0)	36.5 (354.5)	37.1 (359.9)	35.3 (343.7)
22	36.3 (352.7)	37.0 (359.0)	36.2 (351.8)	37.2 (360.8)	35.2 (342.8)
23	35.2 (342.8)	36.8 (357.2)	36.0 (350.0)	36.8 (357.2)	36.3 (352.7)
24	33.2 (324.8)	34.7 (338.3)	36.2 (351.8)	36.2 (351.8)	35.6 (346.4)
25	29.1 (290.8)	33.9 (331.1)	34.7 (338.3)	33.2 (324.8)	33.4 (326.6)
26	26.8 (274.6)	29.1 (290.8)	26.8 (274.6)	23.3 (251.8)	26.0 (269.0)
27	27.1 (276.7)	26.4 (271.8)	26.7 (273.9)	25.1 (262.7)	27.3 (278.1)
27	27.8 (281.6)	24.9 (261.4)	23.6 (253.6)	26.1 (269.7)	28.1 (273.7)
29	28.1 (273.7)	24.4 (258.4)	23.3 (251.8)	26.3 (271.1)	27.3 (278.1)
30	29.0 (290.0)	25.6 (266.2)	23.9 (255.4)	26.4 (271.8)	29.0 (290.0)
31	29.2 (291.6)	26.5 (272.5)	24.8 (260.8)	27.3 (278.1)	28.9 (289.3)
32	29.0 (290.0)	26.6 (273.2)	25.4 (264.8)	26.5 (272.5)	27.3 (278.1)

From the working surface of the head, the structure is deformed; at some points, we see a layer of cold-worked metal (thickness up to 0.065 mm), which has formed as a result of rail operation.

Throughout the profile, the microstructure consists of sorbite and plate pearlite, whose dispersity declines on moving away from the surface. The microstructure of the base in the region of reduced hardness consists of plate and granular pearlite.

CONCLUSIONS

Japanese R65 rail is metallographically analyzed after operation in the East Siberian Railroad. Its chemical composition complies with Technical Specifications TU 0921-239-01124323–2007 for the steel used in the production of 350LDT rail. The macrostructure of the metal is of satisfactory quality. The tensile mechanical properties, hardness, and impact strength at +20°C determined on samples from the

nonoperational chamfer of the rail head are consistent with Technical Specifications TU 0921-239-01124323–2007.

The elevated hardness at the head's contact surface (404 *HB*) and the reduced impact strength at +20°C (8.6–12.0 J/cm^2) for samples cut from the operational chamfer of the rail head are due to cold hardening of the metal surface in operation. The surface hardness of the base is mainly 35.2–37.8 *HRC* (342.8–366.2 *HB*) over the length of the sample. Sections with reduced hardness (23.2–29.2 *HRC* (251.8–291.6 *HB*) are also observed.

The content of nonmetallic inclusions is low. However, exogenous inclusions (globular inclusions of diameter 10 μm) are encountered.

The microstructure of the Japanese rail sample consists of sorbite and plate pearlite, whose dispersity declines on moving away from the surface. In operation of the rail, thin inclined cracks (depth 1.1 mm) form at the surface of the working chamfer in the rail head; in addition, the lateral wear is considerable (up to 15 mm).

REFERENCES

1. Kozyrev, N.A., Pavlov, V.V., Godik, L.A., and Dement'ev, V.P., *Rel'sy iz elektrostali (Rails from Electric Steel), Novokuznetsk*: Novokuznetsk. Poligrafkombinat, 2006.
2. Vinograd, M.I. and Gromova, G.P., *Vklyucheniya v legirovannykh stalyakh i splavakh (Inclusions in Alloyed Steel and Alloys)*, Moscow: Metallurgiya, 1971.
3. Gol'dshtein, Ya.E. and Mizin, V.G., *Inokulirovanie zhelezo-uglerodistykh rasplavov (Inoculation of Iron-Carbon Melts)*, Moscow: Metallurgiya, 1993.
4. Elanskii, D.G., Development tendency of electric steelmaking, *Elektrometallurgiya*, 2001, no. 5, pp. 3–18.
5. Polyakov, V.V. and Velikanov, A.V., *Osnovy tekhnologii proizvodstva zheleznodorozhnykh rel'sov (Bases of Rail Production Technology)*, Moscow: Metallurgiya, 1990.
6. Mengwen, Yu. and Kebing, J., Development of heavy rail production technology at Panzhihua Iron and Steel Company, *Proc. Int. Symp. on Exploitation and Utilization of Vanadium, Panzhihua, China*, Beijing: Metallurgical Industry, 1985, pp. 358–366.
7. Klisiewicz, Z., Wytwarzanie staly na Szyuy o podwyz szonych Wlasnosciach wytuzymalosuowych w Kouwertonach tlenowych z zastosowacuem obnobki prozniowej cieklej stali, *Hutnik*, 1987, vol. 53, no. 3, pp. 62–64.
8. Steel for rails of high-speed lines, *Zhelezn. Dorogi Mira*, 2000, no. 8, pp. 67–70.
9. Spies, H.-J., *Verhalten von Nichtmetallischen Einschlussen im Stahl*, Leipzig, 1968.
10. Shul'te, Yu.A., *Nemetallicheskie vklyucheniya v elektrostali (Nonmetallic Inclusions in Electric Steel)*, Moscow: Metallurgiya, 1964.
11. Shur, E.A., *Povrezhdeniya rel'sov (Rail Damage)*, Moscow: Transport, 1971.
12. Pavlov, V.V., Temlyantsev, M.V., Korneva, L.V., Oskolkova, T.N., and Gavrilov, V.V., *Defekty i kachestvo rel'sovoi stali (Defects and Quality of Rail Steel)*, Moscow: Teplotekhnik, 2006.
13. Lempitskii, V.V., Kazarnovskii, D.S., Gubert, S.V., et al., *Proizvodstvo i termicheskaya obrabotka zheleznodorozhnykh rel'sov (Production and Thermal Treatment of Rails)*, Moscow: Metallurgiya, 1972.
14. Kozyrev, N.A., Production of low-temperature rails, *Steel Transl.*, 2011, vol. 41, no. 4, pp. 287.
15. Snitko, Yu.P., Galyamov, A.Kh., and Nikitin, S.V., Modern state of rail production abroad, in *Materialy yubileinoi rel'sovoi komissii 2002 g. (Proceedings of Jubilee Rail Commission 2002), Novokuznetsk*: Novokuznetsk. Poligrafkombinat, 2002, pp. 10–30.

Translated by Bernard Gilbert